Crystal Unfolding and Chain Disentanglement During Semicrystalline Polymer Dissolution

Surya K. Mallapragada and Nicholas A. Peppas
Polymer Science and Engineering Lab., School of Chemical Engineering, Purdue University,
West Lafayette, IN 47907

Mathematical models developed describe the unfolding of polymeric crystals in the presence of a solvent followed by their subsequent disentanglement. A thermodynamic model considering the free energy changes during crystal unfolding was proposed to obtain an expression for the unfolding rate. A simplified version of this expression, assuming uniform crystal size, was incorporated into a continuum model to predict the dissolution kinetics of a semicrystalline polymer slab. The model yielded predictions of the crystalline and solvent volume fractions as a function of position within the slab, in addition to changes in the fraction of polymer dissolved as well as the degree of crystallinity of the polymer as a function of time. The degree of crystallinity of the polymer decreased with time and the plot of the fraction of the polymer dissolved as a function of time exhibited Case II behavior. The model predictions agreed will with experimental results obtained during dissolution of semicrystalline poly(vinyl alcohol) in water.

Introduction

The dissolution of semicrystalline polymers is important in a number of applications such as recycling of polymers (Nauman and Lynch, 1994), membrane science (Meares, 1987), and in controlled drug delivery (Conte et al., 1988). The polymer dissolution process is preceded by diffusion of solvent into the polymer. However, the diffusion of solvents through semicrystalline polymers has been studied extensively. The diffusion models, however, have not been extended to describe the dissolution process. Three basic approaches have been used for modeling such systems: (i) free volume theories (Kreituss and Frisch, 1981) which assume the crystalline regions to be impermeable and the transport to occur through the amorphous regions; (ii) theories which regard semicrystalline polymers (Michaels and Hausslein, 1965; Fuhrman, 1979) as three-phase systems composed of a noncrystalline matrix, crystallites, and the phase of crystalline interfaces; and (iii) theories based on the idea of entropy correlation (Barker et al., 1978).

Although there has been considerable experimental work on the dissolution of semicrystalline polymers, no models have been proposed to predict the dissolution kinetics. Semicrystalline polymers dissolve by unfolding of the crystal chains (Mallapragada and Peppas, 1996) to join the amorphous portion, followed by subsequent disentanglement (Figure 1). In this work, we have modeled both the crystal unfolding, as well as the disentanglement process during semicrystalline polymer dissolution in order to predict the kinetics of the process.

Unfolding of Crystal Chains

The semicrystalline polymer was assumed to have crystallites formed due to folding of the chains, as shown in Figure

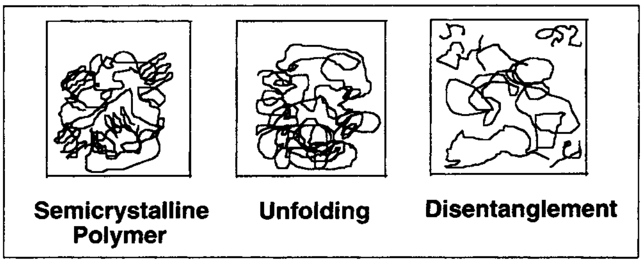

Figure 1. Crystal unfolding and subsequent disentanglement in the presence of a solvent.

Correspondence concerning this article should be addressed to N. A. Peppas.
Current address of S. K. Mallapragada: Dept. of Chemical Engineering, Iowa State University of Science and Technology, Ames, IA 50011.

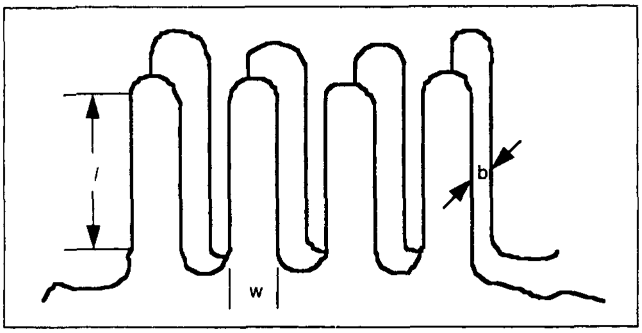

Figure 2. Polymer crystal.

2. The free energy change during chain unfolding depends on the dimensions of the crystal and on the surface energies along different planes in the crystal. After the chains of the crystal unfold and join the amorphous portion surrounding them, they interact with the solvent. The free energy change due to this mixing process is given by the Flory-Rehner equation. This model assumes the absence of hydrogen bonding in the system.

The system was defined using the following parameters. The crystallites were formed by folded polymer chains of lamellar thickness l, width w, distance b between the rows of chains (Figure 2), and have a cross-sectional area a. The lamellar thickness is not the same for all the crystallites, and the average lamellar thickness varies with the conditions of crystallization. Here, Δf denotes the free energy difference per unit volume between the crystalline and amorphous material. The terms σ_e and σ_s are the end surface and the side surface free energies. The parameter ν is the number of successive chains that form a crystal. The parameter $N(\nu, l)$ was defined as the number of crystals of length l in the range l and $l+dl$ and of cross-sectional area $a\nu$. Finally, χ is the polymer-solvent interaction parameter.

Using the above notation and based on the theory of Lauritzen and Hoffman (1960), the free energy change $\Delta G(\nu, l)$ in unfolding a chain of length l, thickness b and width w from a single crystal was written as

$$\Delta G_1 = bwl\,\Delta f - 2bw\sigma_e - 2bl\sigma_s \tag{1}$$

Therefore, the free energy change in a crystal with two rows of chains transforming to one row was given by

$$\Delta G_2 - \Delta G_1 = bw(l\Delta f - 2\sigma_e) \tag{2}$$

Generalizing, the free energy change in going from $\nu+1$ rows to ν rows of chains in a crystal was also given by

$$\Delta G_{\nu+1} - \Delta G_\nu = bw(l\Delta f - 2\sigma_e) \tag{3}$$

The Flory-Rehner theory (Flory, 1953) was used to obtain the free energy change ΔG due to interaction between the unfolded polymer chains and the solvent leading to

$$\Delta G' = (n_1 \ln v_1 + n_2 \ln v_2 + n_1 \chi_1 v_2)\,\mathrm{kT} \tag{4}$$

where v_1 is the volume fraction of the solvent, v_2 is the volume fraction of the polymer in the solution, and n_2 and n_1 are the number of moles of the polymer and the solvent, respectively.

This led to an expression for R_-, the rate at which the crystals in the given length regime l to $l+dl$ unfold one row of chains (that is go from $\nu+1$ rows to ν rows of chains) given by

$$R_-\,dl = N(\nu+1,l)\,dl\exp[-(w_1/\mathrm{kT})]\,\mathrm{kT/h} \tag{5}$$

Here, kT/h is the rate of thermal vibration and $\exp[-(w_1/\mathrm{kT})]$ is the probability that one of these vibrations will cause a "backward" step, that is, unfolding of a row of chains. This equation was based on the absolute rate theory of Glasstone et al. (1941). This probability depends on the free energy changes that occur during the process.

For this case, it can be shown that

$$w_1 = \Delta f^* + 0.5[\Delta G(\nu+1,l) - \Delta G(\nu,l)] + \Delta G' \tag{6}$$

From these, the rate of backward growth of the crystal (that is, unfolding) was obtained as

$$R_-(\nu,l) = N(\nu+1,l)\frac{\mathrm{kT}}{\mathrm{h}}\exp\left(-\frac{\Delta f^*}{\mathrm{kT}}\right)\exp\left(\frac{(\Delta G_{\nu+1} - \Delta G_\nu - 2\Delta G')}{2\mathrm{kT}}\right) \tag{7}$$

As a first approximation, a uniform initial size distribution of the crystals N_0 was assumed. Also, at steady state, all the R values are constant. Thereby, Eq. 7 was treated as a recursion formula for $N(\nu, l)$. Invoking the fact that $N(\nu,l)$ is bounded for large ν, a useful form for the rate of unfolding k_1 was obtained as

$$k_1 = 2\frac{\mathrm{kT}}{h}N_0\exp\left[-\frac{l(b\sigma_s - bw\Delta G) + \Delta G'}{\mathrm{kT}}\right]\exp\left(-\frac{2bw\sigma_e}{\mathrm{kT}}\right)\sinh\left[\frac{bw(l\Delta G - 2\sigma_e) + \Delta G'}{2\mathrm{kT}}\right] \tag{8}$$

Typical values of the parameters in the above equation were obtained from Schultz (1974) as σ_e and σ_s of 100 erg/cm^2 and 10 erg/cm^2, respectively. The term ΔG was calculated by using the following equation (Schultz, 1974)

$$\Delta G = \frac{\Delta h_f(T_m^0 - T)}{T_m^0} \tag{9}$$

where Δh_f is the heat of fusion per unit volume of the polymer, and T_m^0 is the melting point of an infinitely thick crystal. For small values of v_1, it can be shown that Eq. 8 yields a first-order dependence of unfolding rate on v_1. This assumption is justified because the volume fraction of water penetrating the crystal is negligibly small. Thus, from the above equations, a constant value for the unfolding rate k_1 was obtained.

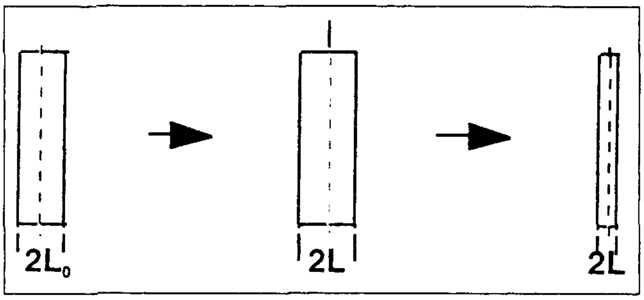

Figure 3. Dissolution of a semicrystalline polymer slab.

Dissolution Kinetics of Semicrystalline Polymers

A model proposed describes the dissolution kinetics by incorporating the constant rate of unfolding derived earlier into a continuum framework involving the dissolution of a semicrystalline polymer slab of half thickness L_0 (Figure 3). This is a moving boundary problem in which the boundary moves outward initially as the polymer slab swells, and then moves inward as the polymer starts dissolving by disentanglement.

The polymer was assumed to be in the rubbery state, that is, the glassy rubbery transition kinetics were assumed to be very fast in comparison to the dissolution kinetics. This is reasonably true for the dissolution of very thin polymer films. The transport was assumed to be one-dimensional. The solvent was envisaged to penetrate the slab causing unfolding of the chains of the crystal, thereby increasing the amorphous portion of the polymer. The three components in the system were the solvent, the amorphous portion of the polymer, and the crystalline portion of the polymer. The suffixes 1, 2a, and 2c refer to the solvent amorphous portion of polymer, and the crystalline portion of the polymer, respectively. Expressions were written for the rates of change of volume fractions v of the various components. The sum of the three volume fractions is always equal to unity.

The expression for rate of change of the crystalline portion is proportional to the unfolding rate k_1 obtained earlier, and the solvent concentration. Therefore, the expression for change in the volume fraction of the crystalline portion of the polymer as a function of time was written as

$$\frac{\partial v_{2c}}{\partial t} = -k_1 v_1 H(v_{2c}) \tag{10}$$

As we have assumed all crystals to be of the same size initially, Eq. 10 is valid. The Heavyside function $H(v_{2c})$ prevents the crystal volume fraction from becoming negative as the crystal unfolding occurs for an extended period. The expression for rate of change of the amorphous portion has a classical diffusion term and an additional source term because of the transformation of the crystalline phase to the amorphous phase during the unfolding process. The diffusion coefficient D was assumed to be dependent on solvent volume fraction according to a Fujita (1961) equation

$$D = D_0 \exp(a_D v_1) \tag{11}$$

Here, D_0 is the self diffusion coefficient of the glassy polymer and a_D represents the steepness of the glassy-rubbery transition. Therefore, the expression for rate of change of v_{2a} with time and with distance from the center of the slab x was given by

$$\frac{\partial v_{2a}}{\partial t} = \frac{\partial}{\partial x}\left(D\frac{\partial v_{2a}}{\partial x}\right) + k_1 v_1 H(v_{2c}) \tag{12}$$

The initial half thickness of the slab was L_0. As the boundary moved, the rate of change of the half thickness of the slab with time was given by

$$\frac{dL}{dt} = -\left(D\frac{\partial v_1}{\partial x}\right)_{x=L} - k_2 v_{2a}\delta(v_{2c}) \tag{13}$$

When the polymer starts dissolving, the movement of the boundary inwards cannot be at a rate that is greater than the rate of unfolding of the chains of the crystal. Therefore, if there are crystals present at the boundary, the boundary does not move inward until all of the crystals unfold. This was mathematically represented by a Dirac delta condition at the boundary which existed only when $v_{2c} = 0$.

The initial and boundary conditions for the system of equations are as follows. Initially, the degree of crystallinity of the polymer is X, and there is no solvent present in the system. Therefore

$$t = 0 \quad -L_0 \le x \le L_0 \quad v_3 = X \quad \text{and} \quad v_2 = 1 - X \tag{14a}$$

$$t = 0 \qquad L = L_0 \tag{14b}$$

A symmetry condition was written at the center of the slab, represented as

$$t > 0 \qquad x = 0 \qquad \frac{\partial v_{2a}}{\partial x} = 0 \tag{15}$$

At the polymer solvent interface, a pseudo-equilibrium assumption was made equating the solvent chemical potential on either side of the boundary. This concentration was estimated by using thermodynamics of swollen networks (Papanu et al., 1989)

$$t > 0 \qquad x = \pm L \qquad \frac{v_{2a}}{1 - v_{2c}} < 1 \tag{16}$$

This completed the formulation of the moving boundary problem. This is a one parameter model as the ratio between the equilibrium concentrations at the polymer solvent interface was maintained constant, and was invariant of molecular weight and crystal-size distribution.

Solution Technique

There are two main techniques to solve moving boundary problems (Crank, 1984). The first technique tracks the moving front, and the second technique fixes the position of the front. The latter was used in this case. Thus, the moving boundary problem was converted to a fixed boundary problem by using a Landau transform given by

$$\xi = \frac{x}{L(t)} \qquad (17)$$

This transformed Eq. 12 to a convective-diffusive form. Equations 10, 12 and 13 were transformed as

$$-\frac{\xi}{L}\frac{dL}{dt}\frac{\partial v_{2c}}{\partial \xi} + \frac{\partial v_{2c}}{\partial t} = -k_1 v_1 H(v_{2c}) \qquad (18)$$

$$\frac{\partial v_{2a}}{\partial t} - \frac{\xi}{L}\frac{dL}{dt}\frac{\partial v_{2a}}{\partial \xi} = \frac{1}{L^2}\frac{\partial}{\partial \xi}\left[D\frac{\partial v_{2a}}{\partial \xi}\right] + k_1 v_1 H(v_{2c}) \qquad (19)$$

$$\frac{dL}{dt} = -\left(\frac{D}{L}\frac{\partial v_1}{\partial \xi}\right)_{\xi=1} - k_2 v_{2a}\delta(v_{2c}) \qquad (20)$$

The boundary conditions were also transformed to

$$\xi = 0 \qquad \frac{\partial v_{2a}}{\partial \xi} = 0 \qquad (21)$$

$$\xi = \pm 1 \qquad \frac{v_{2a}}{1 - v_{2c}} < 1 \qquad (22)$$

The system of coupled partial differential equations was solved numerically by a combination of explicit and implicit finite difference techniques. The finite difference algorithm reduced the system to one consisting of nonlinear algebraic equations. These equations were solved using finite difference techniques. For this purpose, the polymer slab was transformed into a grid and v_{2c} and v_{2a} are represented by the symbols v and u, respectively. The x coordinate is represented by the subscript i, which ranges from 0 to 1, and the time by the superscript n. Also, Δx was the spatial step and Δt was the time step used. The transformed equations were written in finite difference form as shown below

$$\frac{v_i^{n+1} - v_i^n}{\Delta t} = \frac{\xi_i^n}{L}\frac{dL}{dt}\frac{v_{i+1}^n - v_{i-1}^n}{2\Delta x} - k_1(1 - v_i^n - u_i^n) \qquad (23)$$

$$\frac{u_i^{n+1} - u_i^n}{\Delta t} = \frac{\xi_i^n}{L}\frac{dL}{dt}\frac{u_{i+1}^{n+1} - u_{i-1}^{n+1}}{2\Delta x} + k_1(1 - v_i^n - u_i^n) + \frac{p_i^n}{L^2}\left[\frac{u_{i+1}^{n+1} - u_i^{n+1} + u_{i-1}^{n+1}}{\Delta x^2}\right] + \frac{q_i^n}{L^2}\left[\frac{u_{i+1}^{n+1} - u_{i-1}^{n+1}}{2\Delta x}\right]^2 \qquad (24)$$

where

$$p_i^n = D_0 \exp(a_D(1 - u_i^n - v_i^n)) \qquad (25)$$

$$q_i^n = a_D p_i^n \qquad (26)$$

$$\frac{L^{n+1} - L^n}{\Delta t} = \frac{1}{L^{n+1}}\left[-p_i^{n+1}\frac{(u_{i+1}^{n+1} - u_{i-1}^{n+1})}{2\Delta x_1}\right] - k_2 v_i^{n+1} \qquad (27)$$

Equation 24 was recast into a tridiagonal form, as represented by Eq. 28 and solved using the Thomas algorithm (Hoffman, 1992)

$$u_{i+1}^{n+1}\left[\frac{\xi_i^n}{L}\frac{dL}{dt}\frac{1}{2\Delta x} + \frac{p_i^n}{L^2\Delta x^2}\right] - u_i^{n+1}\left[\frac{1}{\Delta t} + \frac{p_i^n}{L^2\Delta x^2}\right] + u_{i-1}^{n+1}\left[-\frac{\xi_i^n}{L}\frac{dL}{dt}\frac{1}{2\Delta x} + \frac{p_i^n}{L^2\Delta x^2}\right] = -\frac{q_i^n}{L^2}\left[\frac{u_{i+1}^{n+1} - u_{i-1}^{n+1}}{2\Delta x}\right]^2 - k_1(1 - v_i^n) + u_i^n\left(k_1 - \frac{1}{\Delta t}\right) \qquad (28)$$

Experimental Part

Poly(vinyl alcohol) (PVA) of molecular weight $\overline{M}_n = 64{,}000$ (Elvanol grade, duPont, Wilmington, DE), with a degree of hydrolysis of 99.8% and a polydispersity index of 2.02 was used for the experiments. Details of the experiment are described elsewhere (Mallapragada and Peppas, 1996). Briefly, a 10% (w/v) aqueous PVA solution was cast on siliconized glass plates and dried at 25°C for 5 days to give films of thickness 0.1 mm. The thickness of the films was measured by profilometry. The films were crystallized by annealing at temperatures of 90°C for 30 min.

Samples of dimensions 1 cm × 1 cm were cut from the films prepared earlier and were partially dissolved in 50 mL of deionized water at 45°C. A 50 mL sample of the residual solution was complexed with 25 mL of 0.65M boric acid solution and 3 mL of 0.05M I_2/0.15M KI solution at 25°C. The concentration of the complexed PVA in the solution was obtained by measuring the absorbance of visible light at 671 nm. Using this, the weight of PVA dissolved was calculated.

Samples removed from the solvent at different intervals were immediately analyzed by differential scanning calorimetry (DSC) (Model 2910, TA Instruments, New Castle, DE). DSC was performed at a scanning rate of 10°C/min from 30 to 250°C and for both the partially dissolved as well as the undissolved samples to determine the degree of crystallinity of the polymer.

Results and Discussion

Typical values for the various parameters for a PVA-water system were used in the simulations. The analysis was performed with polymer degrees of crystallinity varying from 30 to 50%. As indicated by Peppas and Merrill (1976), these are typical attainable degrees of crystallinity for PVA. The unfolding rate k_1 was obtained by taking into account the free energy changes during crystal unfolding, as explained earlier, and the value used was $10^{-4}\ \mathrm{s}^{-1}$. The values of D_0 and a_D were obtained from the Fujita (1961) analysis to be $10^{-9}\ \mathrm{m}^2 \cdot \mathrm{s}^{-1}$ and 7, respectively. The value of disentanglement rate was obtained as $10^{-7}\ \mathrm{m} \cdot \mathrm{s}^{-1}$, using molecular arguments (Narasimhan and Peppas, 1996). The typical features of the simulation include profiles for both crystalline, amorphous, and solvent volume fractions as a function of time. In addition, the position of the polymer-solvent interface, the fraction of polymer dissolved, as well as the degree of crystallinity of the polymer were obtained as a function of time.

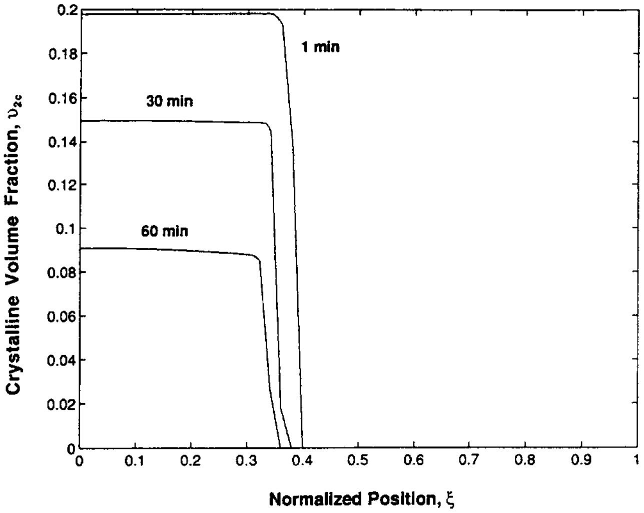

Figure 4. Crystalline volume fraction as a function of normalized half thickness of the slab.

$X = 0.2$; $D_0 = 10^{-9}$ m²/s; $k_1 = 10^{-4}$ s^{-1}; $k_2 = 10^{-8}$ m/s.

Change in the crystalline volume fraction as a function of time and position for a polymer sample with values of parameters listed above is shown in Figure 4. The position $\xi = 0$ represents the center of the slab and the position $\xi = 1$ represents the polymer-solvent interface. It was observed that the unfolding progressed to a large extent as the solvent penetrated the polymer. When the initial degree of crystallinity was increased to 50%, the solvent penetration and crystal unfolding occurred to a lesser degree due to the presence of a larger number of crystals, which hinder solvent transport through the polymer. This is seen in Figure 5. The effect of the unfolding rate and the disentanglement rate on the dissolution kinetics was studied.

When the unfolding rate was decreased by one order of magnitude (all other parameters remaining the same), the extent of solvent penetration as well as the crystal unfolding reduced even further. This is observed in Figure 6. The solvent volume fraction in the polymer is shown as a function of normalized position (Figure 7). As time progressed, it was observed that the solvent volume fraction in the polymer was higher. By integrating the flux of the dissolving polymer, the fraction of polymer dissolved as a function of time was obtained. In Figure 8, the fraction of polymer dissolved is plotted as a function of time. When the disentanglement rate was increased by a factor of ten, the fraction of polymer dissolved increased (Figure 9). This is because the polymer chains at the polymer-solvent interface go into solution more readily. This is in agreement with the experimental data.

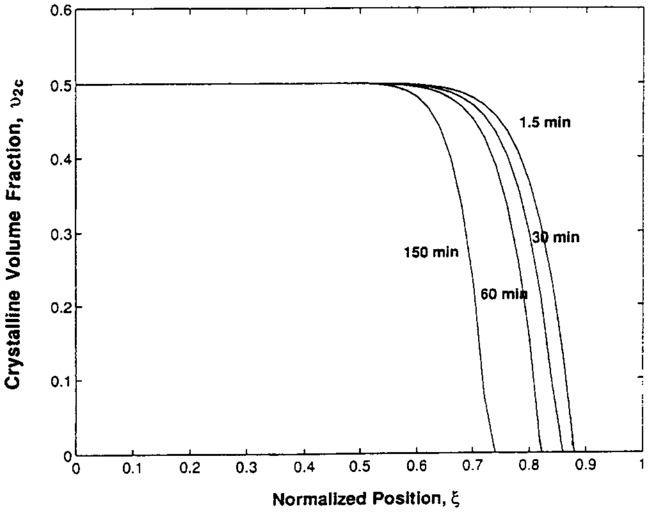

Figure 5. Crystalline volume fraction as a function of normalized half thickness of the slab.

$X = 0.5$; $D_0 = 10^{-9}$ m²/s; $k_1 = 10^{-4}$ s^{-1}; $k_2 = 10^{-8}$ m/s.

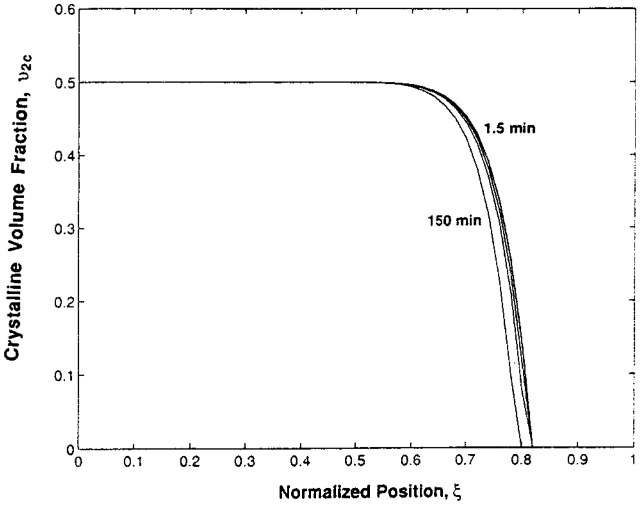

Figure 6. Crystalline volume fraction as a function of normalized half thickness of the slab.

$X = 0.5$; $D_0 = 10^{-9}$ m²/s; $k_1 = 10^{-5}$ s^{-1}; $k_2 = 10^{-8}$ m/s.

A typical plot of the weight of polymer dissolved as a function of time is shown in Figure 10. Case II behavior is ob-

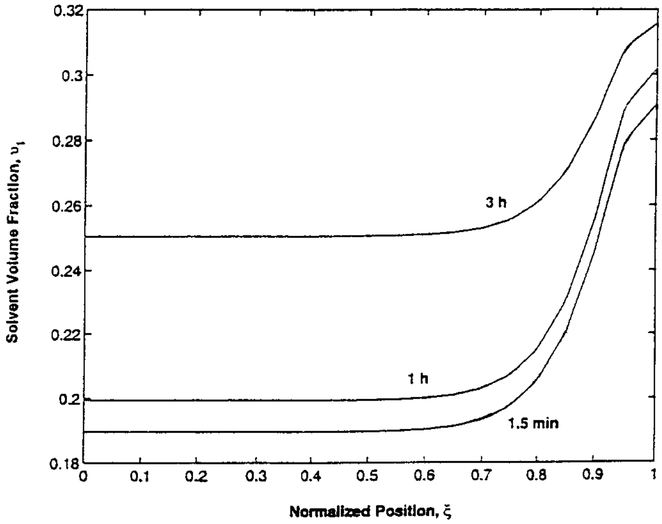

Figure 7. Solvent volume fraction as a function of normalized half thickness of the slab.

$X = 0.5$; $D_0 = 10^{-9}$ m²/s; $k_1 = 10^{-4}$ s^{-1}; $k_2 = 10^{-8}$ m/s.

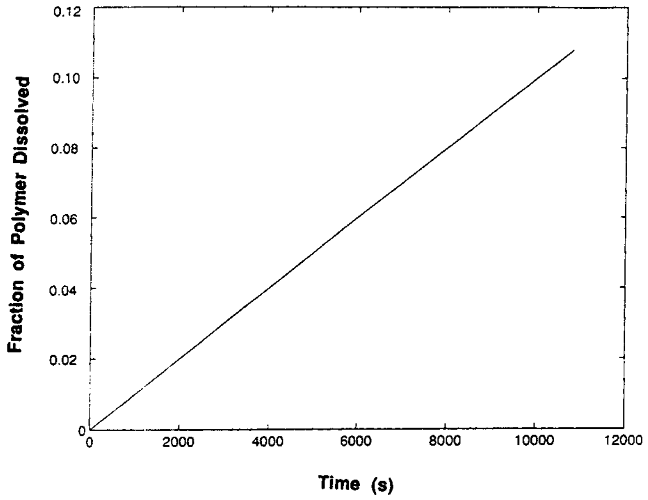

Figure 8. Fraction of polymer dissolved as a function of time.

$X = 0.5$; $D_0 = 10^{-9}$ m²/s; $k_1 = 10^{-4}$ s^{-1}; $k_2 = 10^{-9}$ m/s.

served here, which is similar to the model predictions. Typically, Case II behavior is characterized by a linear behavior between the fraction of polymer dissolved and time, in addition to the boundary advancing at a constant velocity. The heat required for melting the sample was obtained by integrating the area under the melting peak and correcting for the water present in the sample. The melting was seen to occur over a range of temperatures from 190 to 235°C. The heat required for melting a 100% crystalline PVA (Peppas and Merrill, 1976) is 138.6 J/g. Thus, the degrees of crystallinity of the sample were calculated.

Table 1 compares the theoretical predictions of the model with experimental values of the degree of crystallinity of a PVA sample ($\overline{M}_n = 64{,}000$) dissolved in deionized water at 45°C. The values of the parameters used are: $D_0 = 10^{-9}$ m²/s, $a_D = 7$, $k_1 = 10^{-4}$ s^{-1}, and $k_2 = 10^{-8}$ m/s. These values are estimates for PVA of molecular weight $\overline{M}_n = 64{,}000$. Good agreement is observed between the theoretical predictions and the experimental data.

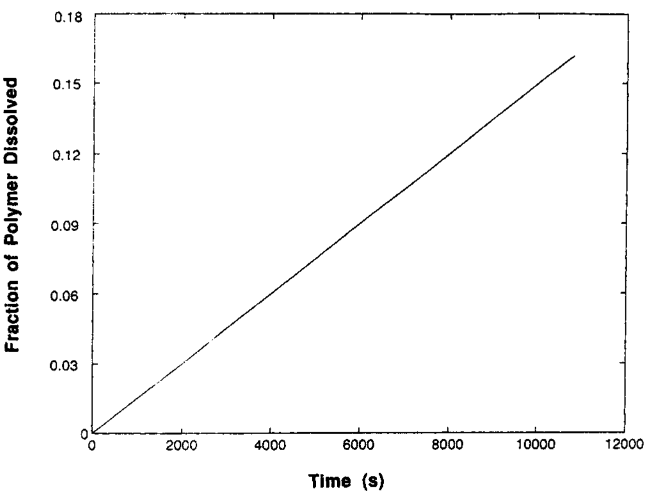

Figure 9. Fraction of polymer dissolved as a function of time.

$X = 0.5$; $D_0 = 10^{-9}$ m²/s; $k_1 = 10^{-4}$ s^{-1}; $k_2 = 10^{-8}$ m/s.

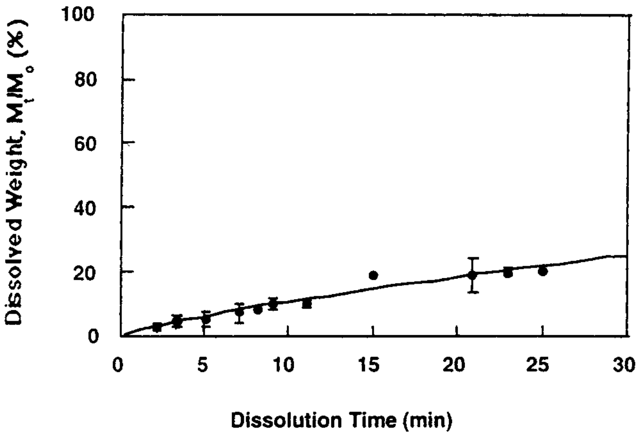

Figure 10. Fraction of PVA dissolved as a function of time for a sample of molecular weight $\overline{M}_n$ = 48,240 crystallized at 110°C for 20 min and dissolved at 30°C.

Table 1. Theoretical Predictions vs. Experimental Values of Degrees of Crystallinity of PVA ($\overline{M}_n$ = 64,000) Dissolved in Deionized Water at 45°C

Dissolution Time (min)	Exp. Deg. of Crystallinity (%)	Pred. Deg. of Crystallinity (%)
0.0	45.0	45.0
1.5	19.0	19.1
30.0	11.1	12.2
60.0	9.1	10.3
150.0	8.3	6.9

Conclusions

Based on a dissolution mechanism for semicrystalline polymers, whereby crystals unfold in the presence of a solvent to join the amorphous portion around them and subsequently disentangle, mathematical models were proposed to describe this process. A free energy based model accounted for the crystal unfolding and was incorporated into a kinetic model to predict the dissolution kinetics of semicrystalline polymers.

The model predictions showed Case II behavior for the fraction of PVA dissolved as a function of time, which was the behavior obtained experimentally too. The degree of crystallinity of the polymer was found to decrease drastically in the presence of the solvent, which showed good agreement with experimental results obtained for the dissolution of PVA in water. Hence, a simplified model, such as the present one, gave reasonable predictions of the dissolution behavior of semicrystalline polymers.

Acknowledgments

This work was supported by grant No. CTS 92-12482 from the National Science Foundation and a Purdue University Global Initiative Grant. We wish to thank Professor Gianni Astarita of the University of Naples for valuable suggestions.

Literature Cited

Barker, R. E., R. C. Tsai, and R. A. Willency, "Entropy Correlation Theory and Diffusion Measurements for Oriented Polymers," *J. Poly. Sci.*, **63**, 109 (1978).

Conte, U., P. Colombo, A. Gazzaniga, M. E. Sangalli, and A. La Manna, "Swelling Activated Drug Delivery Systems," *Biomaterials*, **9**, 489 (1988).

Crank, J., *Free and Moving Boundary Problems*, Oxford Univ. Press, New York (1984).

Flory, P. J., *Principles of Polymer Chemistry*, Cornell Univ. Press, Ithaca, NY (1953).

Fuhrmann, J., "Diffusion in Semicrystalline Polymers and Polymer Networks," *Ber. Bunsenges. Phys. Chem.*, **83**, 303 (1979).

Fujita, H., "Diffusion in Polymer-Diluent Systems," *Fortschr. Hochpolym.-Forsch.*, **3**, 1 (1961).

Gibbs, J. H., *Collected Works*, Longman Green & Co., Essex, U. K. (1928).

Glasstone, S., K. J. Laidler, and H. Eyring, *The Theory of Rate Processes*, McGraw Hill, New York (1941).

Hoffman, J. D., *Numerical Methods for Engineers and Scientists*, McGraw Hill, New York (1992).

Kreituss, A., and H. L. Frisch, "Free Volume Estimates in Heterogeneous Polymer Systems: I. Diffusion in Crystalline Ethylene-Propylene Copolymers," *J. Poly. Sci., Poly. Phys. Ed.*, **19**, 1 (1981).

Lauritzen, J. I., and J. D. Hoffman, "Theory of Formation of Polymer Crystals with Folded Chains in Dilute Solution," *J. Res. Nat. Bur. Std.*, **64A**, 73 (1960).

Mallapragada, S. K., and N. A. Peppas, "Dissolution Mechanism of Semicrystalline Poly(vinyl alcohol) in Water," *J. Poly. Sci.: Poly. Phys.*, **34**, 1339 (1996).

Meares, P., "The Manufacture of Microporous Membranes and Their Structure and Properties," *J. Chem. Tech. Biotechnol.*, **37**, 189 (1987).

Michaels, A. S., and R. W. Hausslein, "Elastic Factors Controlling Sorption and Transport Properties of Polyethylene," *J. Poly. Sci.*, **C10**, 61 (1965).

Narasimhan, B., and N. A. Peppas, "Disentanglement and Reptation During Dissolution of Rubbery Polymers," *J. Poly. Sci., Poly. Phys. Ed.*, **34**, 941 (1996).

Nauman, E. B., and J. C. Lynch, "Polymer Recycling by Selective Dissolution," U.S. Patent 5,278,282 (1994).

Papanu, J. S., D. S. Soane, A. T. Bell, and D. W. Hess, "Transport Models for Swelling and Dissolution of Thin Polymer Films," *J. Appl. Poly. Sci.*, **38**, 859 (1989).

Peppas, N. A., and E. W. Merrill, "Poly(vinyl alcohol) Hydrogels: Reinforcement of Radiation-Crosslinked Networks by Crystallization," *J. Poly. Sci.*, **14**, 441 (1976).

Schultz, J. M., *Polymer Materials Science*, Prentice Hall, Englewood Cliffs, NJ (1974).

Manuscript received June 24, 1996, and revision received Sept. 27, 1996.